Check for updates

Comparative seasonality of phytoplankton community in two contrasting temperate estuaries on the western coast of Korea

Dongyoung Kim[1†], Je Won Sung[1†], Tae-Hoon Kim[2],
Hyung-Mi Cho[3], Jeonghyun Kim[4] and Hyun Je Park[1*]

[1]Department of Marine Bioscience, Gangneung-Wonju National University, Gangneung, Republic of Korea,
[2]Department of Oceanography, Chonnam National University, Gwangju, Republic of Korea, [3]Department of
Ocean Sciences, Inha University, Incheon, Republic of Korea, [4]Department of Earth and Marine Sciences,
Jeju National University, Jeju, Republic of Korea

In estuaries, freshwater discharge functions as a regulator of physicochemical
and biological properties. We assessed the seasonal variability of the
phytoplankton community in response to hydrological features and nutrient
dynamics in two contrasting estuaries in the presence and absence of a dam on
the western coast of Korea. Diversity and evenness were also evaluated through
chemotaxonomic analysis. Seasonal and inter-estuarine comparisons revealed
the overall predominance of diatoms in all seasons and the differentiated
composition of small phytoplankton populations in each estuary, which was
mainly characterized by significant contribution of cryptophytes in the
continuously flushed estuary in contrast to the seasonal occurrence of
pelagophytes and cyanobacteria in the intermittently perturbed estuary. Our
one-way analysis of similarity and similarity percentage analysis showed obvious
inter-estuarine discrepancy of the phytoplankton community in winter in relation
to the high dissolved inorganic nitrogen concentration in the natural estuary,
implying that the impact of freshwater inflow on the phenological response of
phytoplankton can be maximized during active seawater intrusion in dry seasons
in the prevalence of freshwater and seawater in the estuary. The contribution
swing of diatoms and cryptophytes during the study period reflects the seasonal
variability in nutrient dynamics, including absolute concentrations and
stoichiometric ratios, which is especially associated with P-limitation on the
western coast of Korea. The occurrence of cyanobacteria with a summer peak of
phytoplankton biomass in the dammed estuary during the study period indicates
the role of an estuarine dam as a conduit transporting phytoplankton and
dissolved inorganic nutrients. These findings further suggest that the
phytoplankton community structure, differentiated by the presence and
absence of dams, influences bottom-up regulation and thus the food web
structure in estuaries.

KEYWORDS

phytoplankton, freshwater discharge, estuarine dam, photosynthetic pigments,
macrotidal estuary, Han river estuary, Yeongsan river estuary

1 Introduction

Phytoplankton plays a critical role in marine ecosystems as the primary source of organic matter, fueling the biological and geochemical processes in the ecosystem (Mallin et al., 1991; Gomez et al., 2019). The community structure of phytoplankton occurs because of species succession in response to complex environmental conditions (e.g., light, nutrients, hydrography, and zooplankton grazing) in ambient water (Jäger et al., 2008; Estrada et al., 2014). These abiotic and biotic factors vary through seasonal and spatial scales, thereby determining the community structure of phytoplankton in the water column (Smayda and Reynolds, 2001; Prowe et al., 2012). At the interface between the river mouth and the sea, an estuary is distinct coastal water considered a conduit that influences the variability of nutrients, organic matter, and sediments (Pritchard, 1967; Elliott and McLusky, 2002). The physical functioning of estuaries differs and is influenced by factors such as size, shape, sediment properties, and external physical forcings such as tides, waves, wind, and the river (Wolanski and Elliot, 2016). Due to its proximity to human populations, an estuary is typically exposed to anthropogenic forcings such as the input of nutrients and pollutants through the river mouth, causing eutrophication in the estuary (Paerl, 2006). Furthermore, in the case of climate forcing, there is uncertainty about whether the seasonality of precipitation affects hydrodynamic characteristics across and within an estuary. Nowadays, hydraulic structures (e.g., dams and tidal weirs) are impounded in estuaries for various purposes, including flood control, water supply, tidal intrusion prevention, and hydroelectric power generation (Morris, 2013). Discontinuity in the river continuum in the lower estuary may impact the biomass and community structure of phytoplankton (Kim et al., 2023).

On the western coast of Korea, many rivers release substantial amounts of freshwater such as the Han River, the Geum River, and the Yeongsan River. The Han River is the largest in Korea in terms of drainage area (34425.1 km^2) and length (483.0 km) and discharges into the mid-eastern Yellow Sea, penetrating through Seoul City (Water Resources Management Information System, WAMIS, http://www.wamis.go.kr). The Yeongsan River is one of the three major rivers flowing into the western coast of Korea with a 3469.7-km^2 drainage area and 136.0-km length (WAMIS). The discharge of these rivers is mainly concentrated during the summer monsoon period with heavy rainfall (50%–60% of the annual precipitation) from late June to early August (Choi et al., 2020). In the summer, the tidal mixing front expands to 50 km from the coast due to the impact of freshwater discharge from multiple rivers (Seung et al., 1990).

In the Han River estuary (hereafter HRE), although the Singok submerged weir has been constructed to prevent tidal intrusion from the open sea, physical factors (e.g., estuarine circulation, salinity, and freshwater discharge) are unaffected by the weir as freshwater is allowed to flow on the surface (Shin et al., 2019). In the Yeongsan River estuary (Hereafter YRE), an estuarine dam has been constructed to prevent salt intrusion. The dam is regulated by sluice gates that allow freshwater to flow through (Sin et al., 2013). Previous studies have reported the effects of freshwater discharge on

the physiochemical and biological responses in the HRE (Hyun et al., 1999; Youn and Choi, 2008; Yoon and Woo, 2013b) and YRE (Cho et al., 2004; Sin et al., 2013; Hong et al., 2018). However, only a few studies have compared phytoplankton dynamics between continuously flushed (opened) and intermittently perturbed (semi-closed) estuaries in Korea.

Based on the abovementioned difference in physicochemical and morphological conditions, we expected that seasonal successions of the phytoplankton community structure would be distinguishable between continuously flushing estuaries and intermittently perturbed estuaries characterized by macrotidal and shallow coasts in the western region of Korea. To test this hypothesis, we performed seasonal field measurements of photosynthetic pigments (for determination of biomass and chemotaxonomic composition) and physicochemical variables from November 2021 to August 2022. We also estimated the indices of diversity and evenness based on the chemotaxonomic composition to compare the response of the phytoplankton community to environmental differences. Finally, we highlighted the impact of an estuarine dam on the seasonal succession of the phytoplankton community considering the concentrated precipitation and freshwater discharge during the summer monsoon season in a temperate macrotidal estuary.

2 Materials and methods

2.1 Site description and hydrographic sampling

The Yellow Sea, consisting of wide intertidal flats and many islands, is a shallow semi-enclosed sea that has an average depth of 44 m with characteristic tidal amplitudes up to 10 m. The coastal regions of the Yellow Sea are affected by multiple environmental forces, with tide current variability being the most prominent (Hwang et al., 2014). In summer, strong stratification exists deep offshore due to solar heating, in contrast to tidal well-mixing in coastal regions (Kwon et al., 2011).

The HRE and YRE are parts of the Yellow Sea (Figures 1A, B) with mean spring tidal ranges of 5 and 8 m, respectively (Byun et al., 2004). Daily mean discharge rates range from 149 to 2326 m^3 s^{-1} for the HRE (Park et al., 2002) and from 0 to 285 m^3 s^{-1} for the YRE (Park and Sin, 2022). In the HRE, located near Incheon City, the tidal currents are predominantly flood currents toward the upper Han River through the southern channel of the Ganghwa Island during dry seasons, whereas ebb currents prevail toward the open sea through the Yeomha Channel during wet seasons (Yoon and Woo, 2013a; Lee et al., 2021). In the YRE, ebb currents dominate when the tidal flat changes into land, whereas this dominance disappears when the tidal flat changes into sea (Jung and Choi, 2010). In this study, we compared the compositions of phytoplankton in the HRE (in Incheon) and YRE (in Mokpo) by spatiotemporal variations.

Sampling and field observations were performed in November 2021 and February, May, and August 2022 to include four seasons: autumn (November), winter (February), spring (May), and summer (August). To conduct the sample collection in freshwater-affected
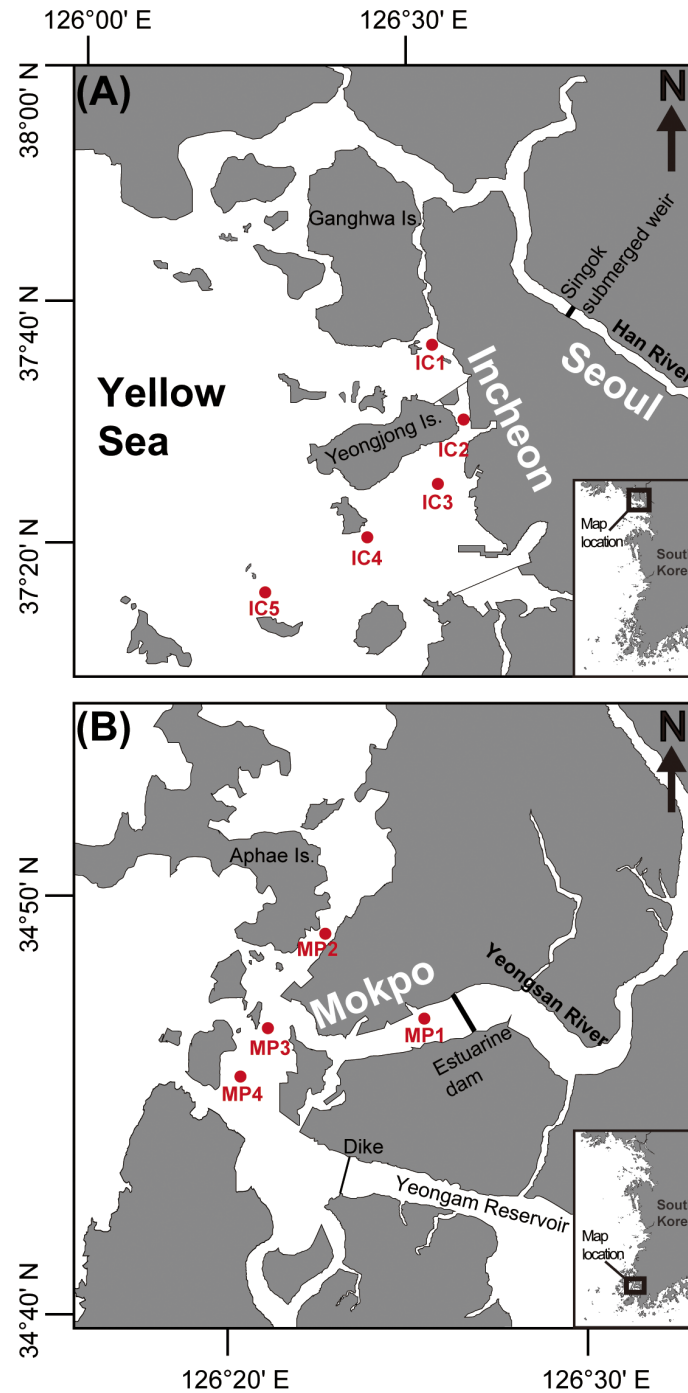
FIGURE 1
Map showing the location of the study area of the Han River estuary (HRE) and Yeongsan River estuary (YRE) off the western coast of Korea.

area, five stations in the HRE (IC1–5) and four stations in the YRE (MP1–4) were determined based on the previous studies (Park et al., 2012; Yoon and Woo, 2015). In each sampling event, the water temperature and salinity were determined *in situ* using a YSI Model 85 probe (YSI Inc., Yellow Springs, OH, USA) and the Secchi and euphotic depths were obtained using a 30-m-diameter circular Secchi disk. A 6-l aliquot of seawater was collected from the sea surface and bottom using a Niskin sampling bottle at each site. The collected water samples were filtered through a 180-μm Nitex mesh net to remove large debris and zooplankton, then immediately transferred in to acid-washed polyethylene bottles and frozen at –20°C. The filter samples were stored at –20°C until photosynthetic analysis.

2.2 Nutrient analysis

The water samples were thawed overnight at a low temperature (2°C) and brought to the laboratory prior to analysis. The

concentrations of nitrate (NO_3^-), nitrite (NO_2^-), ammonium (NH_4^+), silicate [$Si(OH)_4$], and phosphate (PO_4^{3-}) were determined colorimetrically using a QuAAtro nutrient analyzer (SEAL Analytical GmbH, Norderstedt, Germany). The sum of NH_4^+, NO_2^-, and NO_3^- concentrations was considered as the DIN. PO_4^{3-} concentration was considered as the dissolved inorganic phosphorous (DIP), and the $Si(OH)_4$ concentrations was considered as the dissolved silicon (DSi). The measurements were performed in accordance with the Autoanalyzer's practical manuals: NO_3^-, NO_2^-, and DSi (Hansen and Grasshoff, 1983), NH_4^+ (Helder and De Vries, 1979), and DIP (Murphy and Riley, 1962).

2.3 Photosynthetic pigment analysis by high-performance liquid chromatography

To extract photosynthetic pigments, 47-mm Whatman GF/F filters were soaked in 95% methanol (5 ml) at −4°C for 12 h in the dark, then sonicated for 5 min to disrupt the cells, and centrifuged to remove filter debris and cells and aliquots (1 ml) were mixed with 300 μl of water before analysis. A ChroZen high-performance liquid chromatography (HPLC) system (Young-In Chromass, Ahn-yang, Korea) equipped with a Waters Symmetry C8 (4.6 mm × 150 mm; 3.5-μm particle size; 100-Å pore size) column (Waters, Milford, MA, United States) was used to determine photosynthetic pigments according to Zapata et al. (2000). The data matrix included concentrations of diagnostic biomarker pigments: peridinin, 19′-butanoyloxy-fucoxanthin, fucoxanthin, 19′-hexanoyloxy-fucoxanthin, neoxanthin, prasinoxanthin, violaxanthin, alloxanthin, lutein, zeaxanthin, Chl b (DHI, Denmark.), and Chl a (Sigma Co.) The concentration of standard pigments was determined using the absorption coefficients from Jeffery et al. (1997), and absorbance was calculated by adjusting absorbance values using the method described by Park and Park (1997). The pigments were quantified to analyze the community structure of phytoplankton using CHEMTAX by Mackey et al. (1996), based on the relative ratio of Chl a and pigments.

2.4 Chemotaxonomic analysis of phytoplankton groups

The abundance of individual phytoplankton groups was relative to total chlorophyll a (hereafter Chl a) in each water sample and was calculated using CHEMTAX (v. 1.95; https://cmr.earthdata.nasa.gov/search/concepts/C1214308429-AU_AADC) to obtain the phytoplankton composition from HPLC pigment data (Mackey et al., 1996; Wright et al., 1996). The steepest descent algorithm was used to optimize biomarker pigment-to-Chl a ratios to calculate the concentration of Chl a attributed to each class in the phytoplankton community. Previously published biomarker pigment-to-Chl a ratios for phytoplankton classes collected around the Korean peninsula were applied to initial pigment ratio matrices (Supplementary Table 1) and corrected iteratively using CHEMTAX to minimize the sums of squares of differences between observed and

calculated pigment concentrations (Lee et al., 2011). Eight different phytoplankton groups, namely, prasinophytes, chlorophytes, prymnesiophytes (typically coccolithophores), pelagophytes, dinoflagellates, cryptophytes, cyanobacteria, and diatoms, were uploaded for an initial CHEMTAX configuration. The data matrix included concentrations of diagnostic biomarker pigments: peridinin, 19′-butanoyloxy-fucoxanthin, fucoxanthin, 19′-hexanoyloxy-fucoxanthin, neoxanthin, prasinoxanthin, violaxanthin, alloxanthin, lutein, zeaxanthin, and Chl b. The final results were obtained in terms of the absolute concentrations (μg l^{-1}) of Chl a attributed to each phytoplankton class in a sample. Chl a concentrations estimated from CHEMTAX analysis were standardized (convert to percentile value) to calculate their relative portions, which were logarithmically transformed to allow the least abundant groups to contribute to the analysis.

2.5 Group diversity and evenness index

From the percentile contribution of each phytoplankton obtained by CHEMTAX, we calculated phytoplankton group diversity and evenness using the Shannon–Weaver Diversity index (H') and Pielou's evenness index (j'), respectively (Pinckney et al., 2020).

2.6 Statistical analysis

Non-metric multidimensional scaling (nMDS) ordination was performed to unveil seasonal and spatial patterns in the phytoplankton community structure using the contributions of each phytoplankton to total Chl a obtained through CHEMTAX analysis. The percentile contributions of phytoplankton were transformed to log (X + 1) before the estimation of Bray–Curtis similarities (Bray and Curtis, 1957), and one-way analysis of similarity (ANOSIM) was used to analyze differences between phytoplankton classes due to spatiotemporal variations. The output of the test is the "Global R" (if Global R > 0, there is a separation between groups; if Global R < 0, there is no separation between groups). Similarity percentages (SIMPER) were used to identify classes that contributed to the differences in the composition of phytoplankton in each spatiotemporal class to support the ANOSIM results. PRIMER (v. 6.0) was used to conduct SIMPER and ANOSIM analyses. Prior to conducting statistical analyses, the normality of data was tested using the Shapiro–Wilk test and the homogeneity of variance was tested using Levene's procedure. The Kruskal–Wallis nonparametric test was used to compare the seasonal and spatial distributions, followed by Dunn's *post hoc* multiple pairwise comparison. ANOVA test was used to compare the spatial difference of phytoplankton alpha indices between the estuaries. These tests were conducted using IBM SPSS statistics software (v. 22.0, IBM Corp., Armonk, NY). Canonical correspondence analysis (CCA) was performed to visualize the relationships between the variability of the eight phytoplankton groups and biomass (expressed in terms of Chl a concentration) and physical and biogeochemical parameters

(temperature, salinity, density, NO_3^-, NH_4^-, DSi, and DIP concentrations, and stoichiometric ratios among nitrogen, phosphorus, and silicate). A subsequent Monte Carlo permutation test was conducted to evaluate the statistical significance of the CCA results. CCA was performed using CANOCO statistical software (v. 4.5) (Ter Braak and Smilauer, 2002).

3 Results

3.1 Phytoplankton community dynamics

nMDS was performed based on the contribution of the eight phytoplankton groups to total Chl *a*, and the similarities of community structures were calculated and ordinated to visualize the spatiotemporal variations with the 0.17 stress (Figure 2A). The nMDS approach showed that the symbols for autumn observations in the HRE and YRE overlapped in the plot, whereas the symbols for winter observations were plotted with spatial differences. The symbols representing the observations in August 2022 were located without spatial differences between the two estuaries.

The ANOSIM test confirmed the seasonal and spatial dynamics of the phytoplankton communities in the HRE and YRE (HRE: Global R = 0.680, $P = 0.001$; YRE: Global R = 0.592, $P = 0.001$). Positive Global R values were obtained in both the seasonal and inter-estuarine comparisons during the study period (Figure 2B). The pairwise tests showed that phytoplankton communities in the HRE and YRE changed throughout the seasons ($P < 0.01$) (solid arrows in Figure 2B). The Global R value was high in the autumn–winter transition in the HRE (Global R = 1.000, $P < 0.001$), whereas the highest value was obtained between spring and summer in the YRE (Global R = 0.475, $P < 0.01$). Each of the four seasons in the

two estuaries was characterized by different phytoplankton structures (SIMPER results; Figure 2B). Diatoms and cryptophytes were the phytoplankton groups contributing to the seasonal variation in the average dissimilarities of phytoplankton community structures in the HRE (>30% in the autumn and winter), whereas various phytoplankton groups contributed to the dissimilarities of phytoplankton community structures in the YRE. The highest and lowest values of average dissimilarity were observed in autumn–winter in the HRE and YRE, respectively.

The spatial comparison using the ANOSIM pairwise test and SIMPER analysis revealed that the phytoplankton community structures in the HRE and YRE were significantly different (dotted arrows in Figure 2B). The inter-estuarine differences were remarkable during winter and summer with high Global R values (>0.5) and average dissimilarity (>30%). The SIMPER analysis revealed that diatoms (45.0%) and cryptophytes (36.1%) contributed the most to the highest average dissimilarity (47.4) in winter, while phytoplankton (diatoms, pelagophytes, and cryptophytes) contributed the least (9.9) in autumn. In spring, there were significant differences between the estuaries ($P < 0.01$) even though the phytoplankton groups were not separated (Global R < 0.5). The ANOSIM and SIMPER tests indicated that the seasonal succession of the phytoplankton community structure did not follow the coincident temporal pattern in the four seasons ($P < 0.01$).

The percentile contribution of the eight phytoplankton groups evidenced the differences between the continuously flushed HRE and the intermittently perturbed YRE, with diatoms being a highly dominant phytoplankton group contributing to the total Chl *a* in both HRE (60.3 ± 19.0%) and YRE (75.6 ± 17.8) (Figure 3). Several seasonal differences were observed, including a higher contribution of cryptophytes from winter to summer (19.5 ± 16.0%) in the HRE and high contributions of pelagophytes,
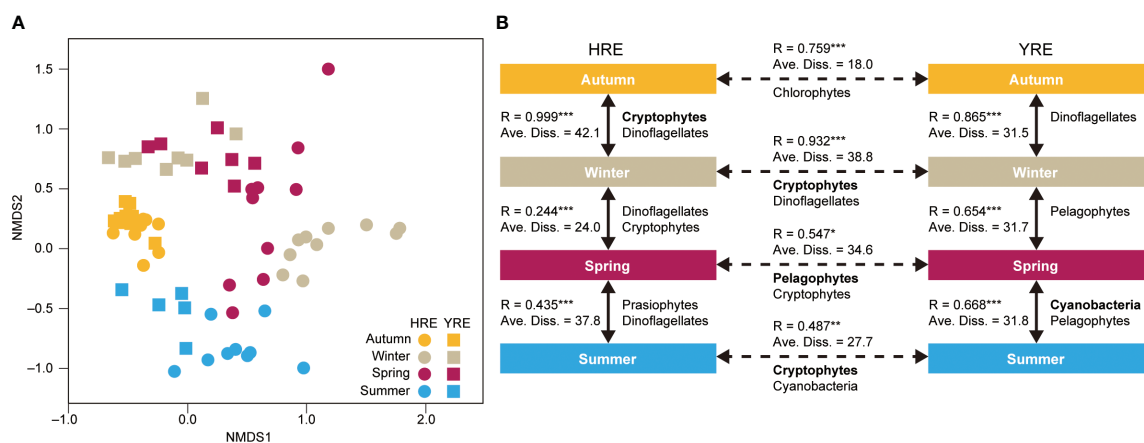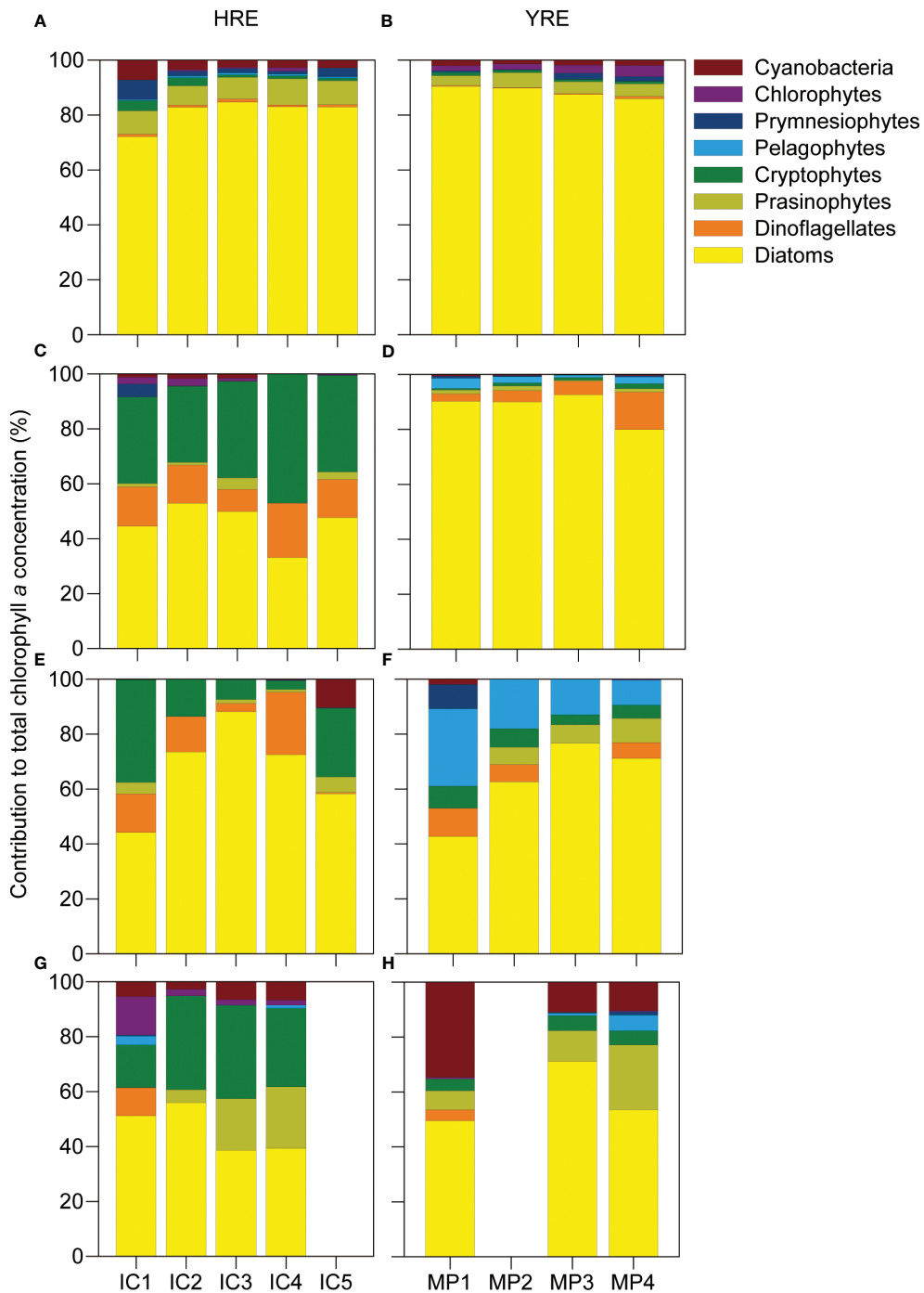

FIGURE 2
(A) Nonmetric multidimensional scaling analysis of phytoplankton groups based on the percentile contribution of eight phytoplankton groups to total chlorophyll a (Chl a) concentration during the study period. Samples obtained in the HRE and YRE are represented by circles and squares, respectively. **(B)** Schematic summary of the results of the analysis of similarities and similarity percentages. Each of the individual figures represents the season during the study period when the percentile contribution of the phytoplankton group is significantly different. Spatiotemporal comparisons between phytoplankton groups are shown in solid arrows (seasonal comparison) and dotted arrows (spatial comparison). Only phytoplankton groups that contributed more to dissimilarity (contribution >10%) are presented. Bolds indicate the phytoplankton groups with the most contribution to dissimilarity >30%. Significance: *0.01 < P < 0.05; **0.001 < P < 0.01; ***P ≤ 0.001.

FIGURE 3
Percentile contribution of eight phytoplankton groups to total Chl *a* concentration in the HRE (left panels) and YRE (right panels) during autumn **(A, B)**, winter **(C, D)**, spring **(E, F)**, and summer **(G, H)** calculated by CHEMTAX. Missing observations of IC5 and MP2 in summer were attributable to unfavorable weather condition during the sampling time.

cyanobacteria, and prasinophytes with gradual increments toward the open sea in spring (pelagophytes: 17.4 ± 11.4%) and summer (cyanobacteria: 18.7 ± 14.4%; prasinophytes: 13.3 ± 7.0%) in the YRE.

3.2 Hydrographic conditions

During the study period, daily precipitation in neighboring cities ranged from 0 to 207.8 mm in Incheon City (for the HRE) and 0 to 81 mm in Mokpo City (for the YRE), with summer

precipitation (June–August) being noticeably higher (Figures 4A, B). The daily discharge rate of the Singok submerged weir and the Yeongsan estuarine dam during the study period varied between 0 and 51.8×10^3 m^3 s^{-1} for the HRE and 0 and 32.5×10^3 m^3 s^{-1} for the YRE, with higher rates during the summer months (June–August) and highest frequencies in August (Figures 4C, D).

Seasonal variations in the seawater temperature exhibited typical patterns in the temperate coastal zone, with higher values

in summer and lower values in winter (2.1°C–27.9°C in the HRE and 4.7°C–28.7°C in the YRE) (Figures 4E, F). Temperature and Salinity variations exhibited seasonal and spatial differences between the two estuaries (Figures 4G, H). In the HRE, the salinity gradient ranged from 1.2 to 31.4, with an obvious gradient depending on the distance from the Han River mouth in autumn, spring, and summer, whereas the salinity gradient was weak in winter. Distinguishably, the polyhaline zone was observed

FIGURE 4
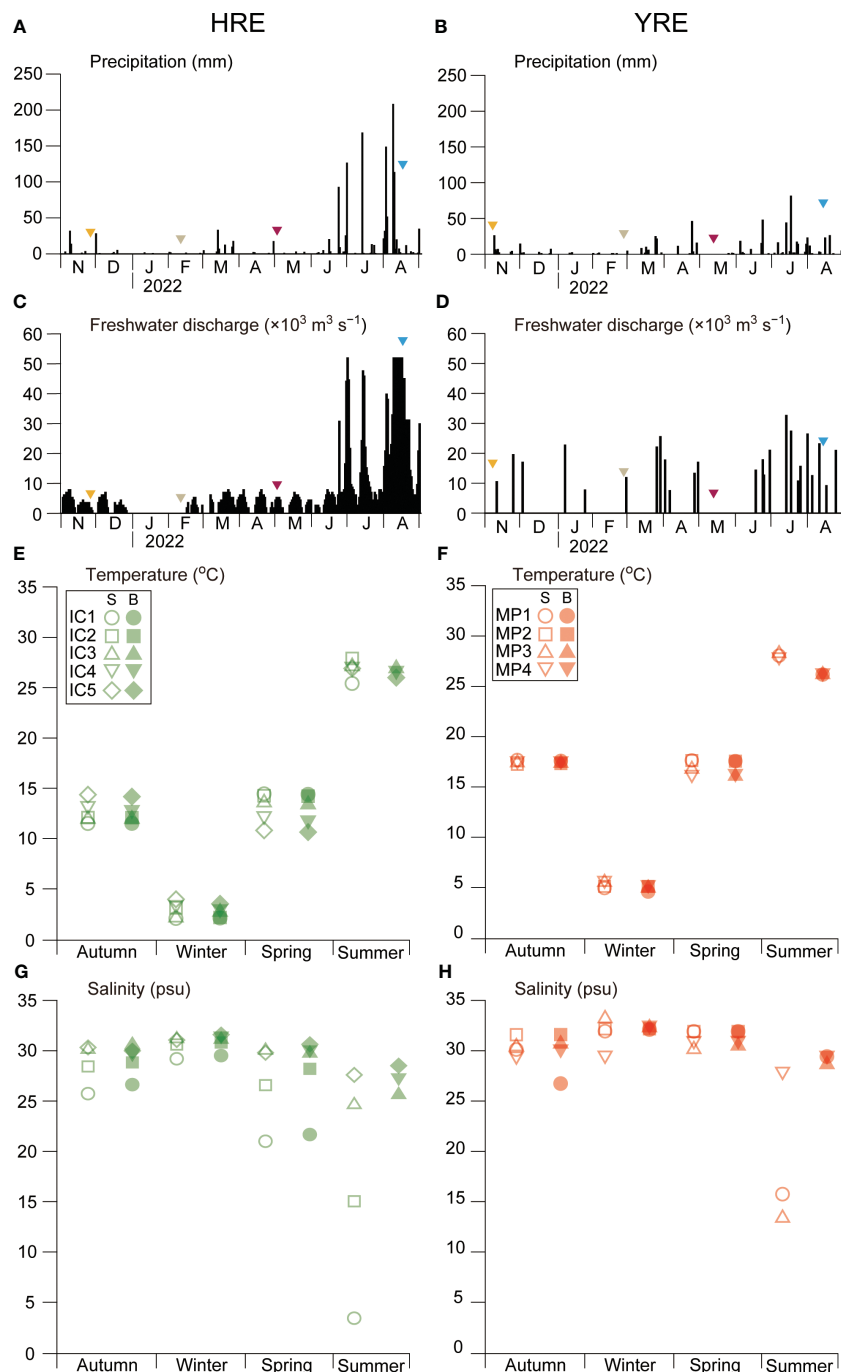Seasonal variations in precipitation in the neighboring land areas [(A) Incheon Metropolitan City and (B) Mokpo City]; mean freshwater discharge of the submerged weir in the Han River (C) and Yeongsan River dam (D); seawater temperature in the HRE (E) and YRE (F); salinity in the HRE (G) and YRE (H) during the study period. S and B indicate the samples collected in surface and bottom, respectively.

in the YRE, while the mesohaline zone was formed in the summer. The significant difference of salinity was observed in the HRE during the study period (Kruskal-Wallis, $p < 0.05$).

3.3 Dissolved inorganic nutrients

Temporal and spatial illustrations revealed variations in the distributions of dissolved inorganic nutrients (Figures 5A–J). During the study period, dissolved inorganic nitrogen (e.g. NO_3^-, NO_2^-, and NH_4^+) were under replete and deplete conditions in the HRE and YRE, respectively. The HRE and YRE had no clear spatial differences in DIP and DSi levels.

NO_3^- was the dominant nitrogenous nutrient, with a strong relationship with the dissolved inorganic nitrogen ($NO_3^- + NO_2^- + NH_4^+ = DIN$, $r^2 = 0.99$, $P < 0.001$) concentration, exhibiting an obvious correlation with salinity ($r^2 = 0.61$, $P < 0.001$) during the study period (Figures 5A, B, E, F). The NO_2^- concentration was negligible during the study period. There was no seasonal trend between the NO_3^- and DIN concentrations in the HRE (Kruskal–Wallis, df = 4, $P = 0.418$). The NH_4^+ concentration had a significant seasonal variation, with lower values in spring in both HRE (Kruskal–Wallis, $P = 0.003$, df = 4) and YRE (Kruskal–Wallis, $P = 0.000$, df = 3), but no significant spatial variation in either estuary (Figures 5C, D).

The DSi concentration varied in the HRE, with lower values in spring (Kruskal–Wallis, $P = 0.001$, df = 4), displaying an obvious correlation with salinity (Spearman's rank correlation analysis $r = -0.53$, $P = 0.000$) during the study period (Figures 5G, H). The DIP concentration in the water column exhibited seasonal differences in both estuaries, with lower values in spring (Kruskal–Wallis, $P = 0.002$, df = 4) in the HRE and lower values in winter and spring in the YRE (Kruskal–Wallis, $P = 0.001$, df = 3) (Figures 5I, J). In winter, significant differences in the DSi and DIP concentrations were observed between the HRE and YRE (Kruskal–Wallis, $P < 0.001$), with higher values in the HRE. A positive correlation between DIP and DSi was observed (Spearman's rank correlation analysis, $r = 0.909$, $P < 0.001$) during the study period.

3.4 Depth-integrated chlorophyll *a* concentrations

Depth-integrated Chl *a* ranged from 1.6 to 59.3 and 11.1 to 105.8 µg m^{-2} in the HRE and YRE, respectively (Figure 6). The significant difference of the depth-integrated Chl a between the HRE and the YRE was observed in winter (Mann-Whitney, $p < 0.05$). Biomass of phytoplankton based on the Chl *a* concentration indicated no significant seasonal variation in phytoplankton biomass in the HRE, whereas higher values were obtained in summer (Kruskal–Wallis, $p = 0.03$, df = 3).

3.5 Nutrient limitation

The molecular N:P, Si:P, and Si:N ratios exhibited the stoichiometric limitation of nutrients, determined by the Redfield ratio (e.g., N:P:Si = 16:1:15) (Figure 7). The P-limitation was noticeable in winter in both estuaries and in spring in the YRE (Figure 7A). There was no obvious N-limitation during the study period (Figure 7B). Si-limitation was observed in the outer station in the HRE (IC3–5) (Figure 7C).

3.6 Environmental–biological relationship: CCA

CCA revealed the relationship between environmental parameters and the phytoplankton community structure and biomass in the HRE and YRE during the study period (Figure 8). The first two axes (1 and 2) accounted for 49.6% and 32.7% of the total variance of the phytoplankton groups in relation to environmental factors in the HRE, respectively (Figure 8A). The CCA differentiated the cryptophytes as the group more associated with high DIN and NO_3^- concentrations. Small phytoplankton populations (e.g., chlrophytes, prasinophytes, pelagophytes, and cyanobacteria) were distributed in the same quadrant as summer symbols, with a positive correlation with the Si:N ratio and Chl *a* concentration and a negative correlation with the N:P ratio. The samples collected in spring differed in salinity and DIN concentration. In the YRE, with 50.7% for axis 1 and 33.1% for axis 2, explaining the total variance, the clockwise distribution of symbols follows the typical seasonality of temperature showing higher temperatures in summer and lower temperatures in winter (Figure 8B). There was an obvious distribution of the symbols in the spring samples with a positive relationship with stoichiometric ratios and a negative relationship with DIN.

3.7 Phytoplankton group diversity and evenness

The comparison of indices in phytoplankton diversity and evenness between two estuary revealed the spatial difference during the study period (Table 1). The Shannon-Wiever Diversity Index (H') ranged from 0.48 to 1.51 and from 0.24 to 1.47 in the HRE and YRE, respectively. Pielou's evenness index (j') varied from 0.23 to 0.97 for the HRE, and from 0.13 to 0.81 for the YRE, respectively. A significant difference of indices for diversity and eveness was observed between the two estuaries with a higher value in the HRE (one-way ANOVA, $P = 0.02$).

4 Discussion

Seasonal variability of phytoplankton is in response to the annual climate cycle, and significant year-to-year variability is associated with human activities or shifts in the climate system (Cloern and Jassby, 2010). The results of our study indicate that the seasonal succession of phytoplankton reflects the physicochemical cycle condition on the western coast of Korea following the East Asian monsoon climate, but the phytoplankton community structure differed by the presence or absence of an estuarine dam
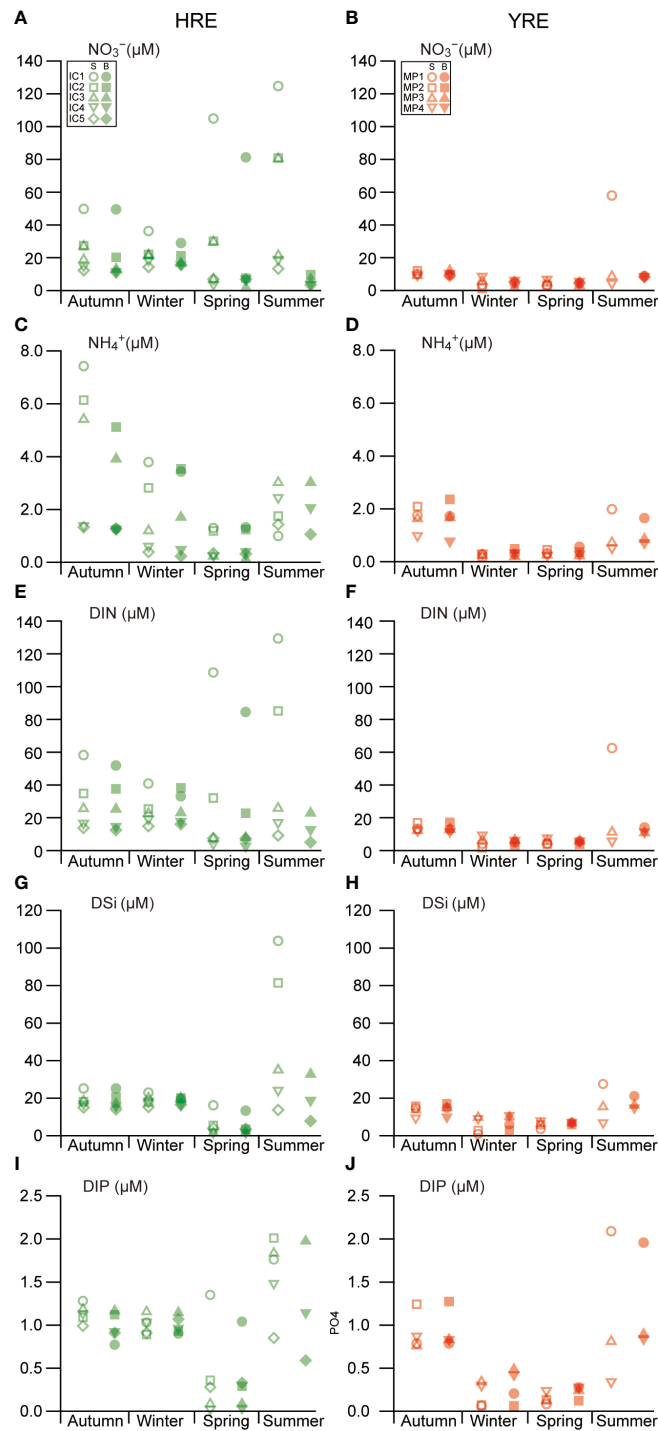
FIGURE 5

Seasonal and spatial variations in dissolved inorganic nutrient concentrations: NO$_3^-$ **(A, B)**, NH$_4^+$ **(C, D)**, DIN **(E, F)**, DSi **(G, H)**, and DIP **(I, J)** concentrations during the study period. S and B indicate the samples collected in surface and bottom, respectively.

regulating the magnitude and timing of freshwater inflow and thus nutrient dynamics (e.g., absolute concentrations and stoichiometric ratios). The decreasing trend of dissolved inorganic nutrients along the salinity gradient without vertical difference in natural estuary (excepting the NH$_4^+$) implys the predominance of freshwater impact compared to the tidal supplement from sediment during the study period. In contrast, the occasional appearance of higher

nutrients in bottom compared to surface might be evidence of tidally supplying mechanism in macrotidal flat. Accordingly the comparative distribution of dissolved inorganic nutrients in vertical and lateral scale can clarify the contrasting environment of estuaries with and without the dam in macrotidal condition. The inter-estuarine comparison of the phytoplankton community structure reveals enhanced dissimilarity in winter, mainly attributed to the
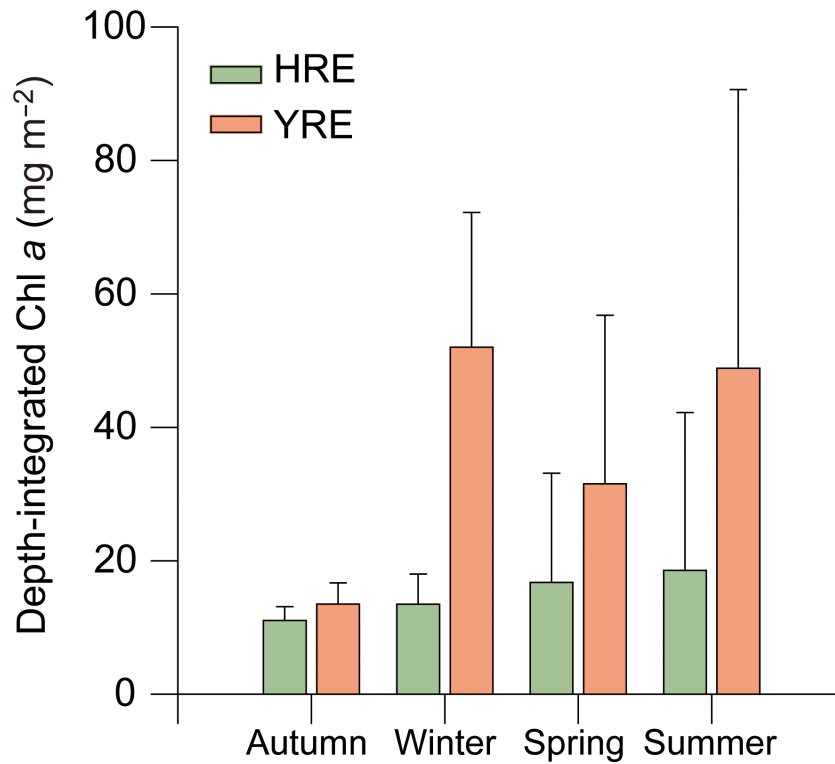
FIGURE 6

Seasonal and spatial variations in Chl *a* and depth-integrated Chl *a* concentrations during the study period.

swing of diatoms and cryptophytes governed by the seasonal prevalence of freshwater inflow and seawater intrusion under macrotidal conditions. Interestingly, the CCA plot indicated that DIN concentrations were not significantly correlated with stoichiometric ratios in the HRE, whereas there was an obvious correlation between nutrient concentrations and their ratios. Accordingly, seasonal and inter-estuarine variability of DIN and swing of diatoms and cryptophytes are essential in understanding ecosystem differences between natural and anthropogenically altered estuaries.

4.1 Contrasts of seasonal/inter-estuarine variability in phytoplankton community structure

Notable characteristics of phytoplankton dynamics in this study were the contrasting seasonality of phytoplankton biomass and community structure between the continuously flushed estuary (the HRE) and the intermittently perturbed estuary (the YRE). Our results indicated no obvious seasonality of Chl *a* concentration in the HRE, contrasting with the summer maxima of Chl *a* in the YRE.
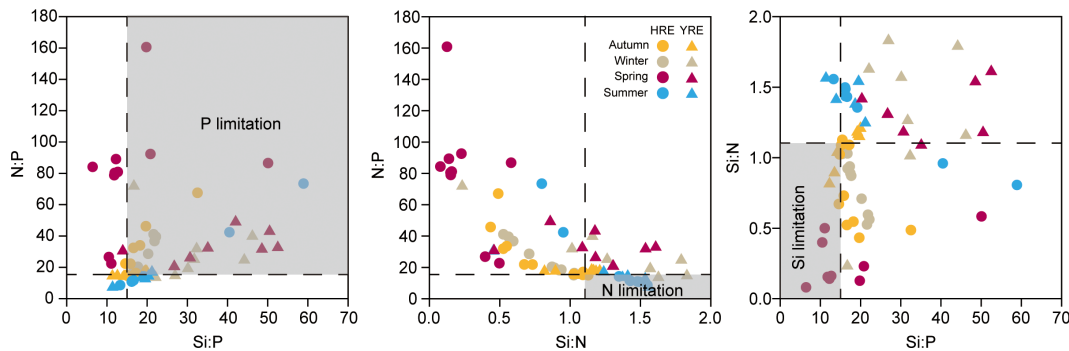

FIGURE 7

Scatter diagrams of molecular nutrient ratios in autumn (yellow), winter (gray), spring (purple), and summer (blue) in the HRE (circle symbol) and the YRE (triangle symbol).
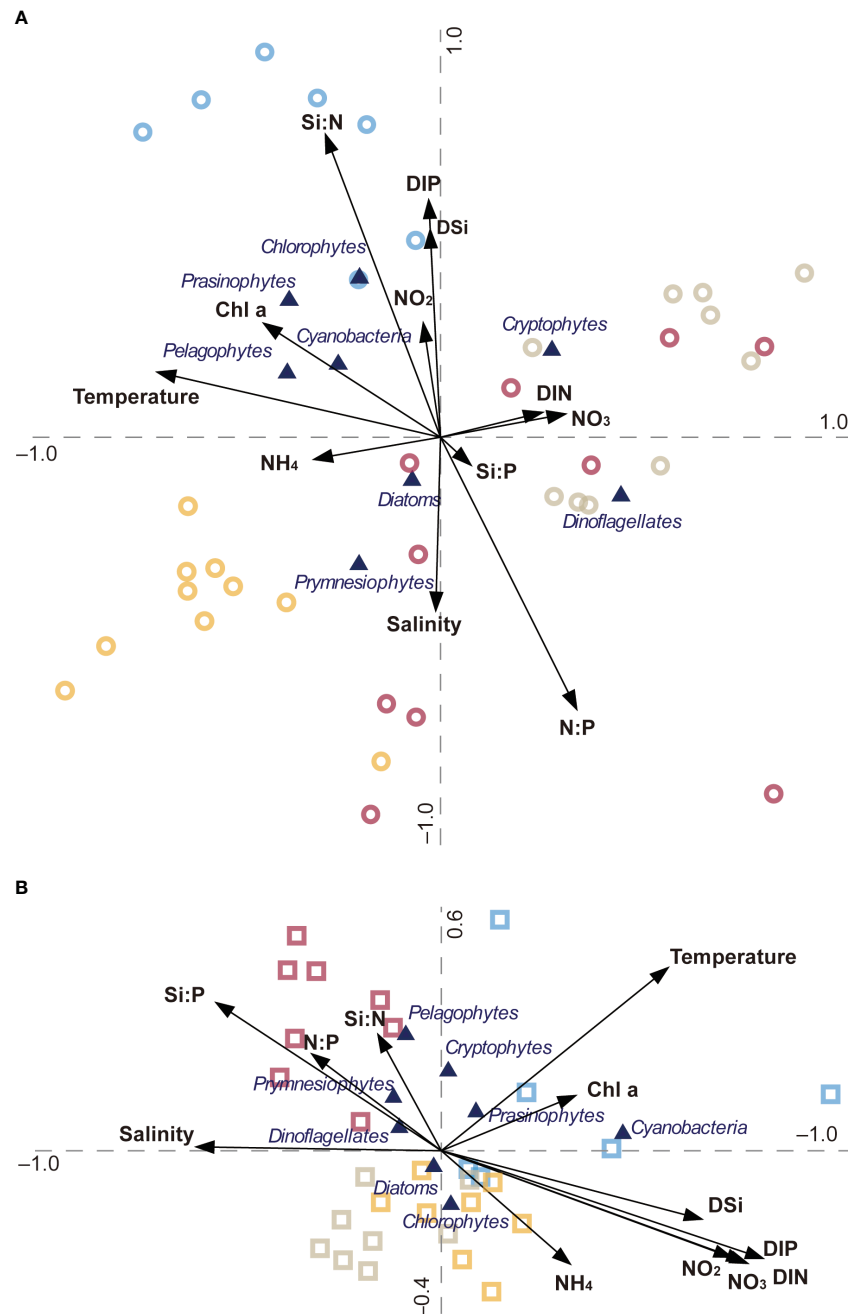
FIGURE 8
Canonical correspondence analysis: ordination diagrams of phytoplankton composition data at various station/season combinations with environmental variables represented by arrows in the panel. Phytoplankton are shown by filled triangles. Samples obtained in the **(A)** HRE and **(B)** YRE are represented by circles and squares, respectively. Seasonal variations in the four seasons are represented as autumn (yellow), winter (gray), spring (purple), and summer (blue).

The positive relationship between salinity and dissolved inorganic nutrients (e.g. NO_3^-, DIN, DIP, and DSi) indicated that continuous river flow formed the eutrophic condition in the HRE. Specifically, our CCA supports the view that the standing stock of phytoplankton in the HRE was not largely responsible for the concentration of nutrients represented by the lower contribution of nitrogenous nutrients (relatively short arrows), showing no obvious relationship with Chl a (See Figure 8A). Accordingly, we can hypothesize that no significant seasonality of phytoplankton

biomass in the HRE was associated with the conservative characteristics of DIN, implying that the vulnerability of the ecosystem was regulated by leading eutrophication by heavy precipitation through freshwater runoff into the macrotidal estuary (Jahan and Choi, 2014). The record-high precipitation in August in adjacent cities (e.g., Seoul and Incheon) may form the polyhaline zone in the upper HRE (Figure 4D). In contrast to the HRE, the summer bloom of phytoplankton was conspicuously characterized by co-dominance of diatoms, cyanobacteria (station

TABLE 1   Phytoplankton alpha diversity indices in the HRE and the YRE during the study period.

Regions	Season	Alpha diversity indices	
		Shannon–Weaver (H′)	Pielou (j′)
HRE	Autumn	0.75 ± 0.14	0.38 ± 0.08
	Winter	1.14 ± 0.17	0.72 ± 0.18
	Spring	0.78 ± 0.25	0.57 ± 0.24
	Summer	1.07 ± 0.35	0.76 ± 0.06
YRE	Autumn	0.53 ± 0.09	0.26 ± 0.04
	Winter	0.46 ± 0.18	0.23 ± 0.09
	Spring	1.06 ± 0.24	0.64 ± 0.10
	Summer	1.04 ± 0.3	0.61 ± 0.13
K-S test		0.857	0.236
ANOVA	HRE × YRE	0.018	0.002

Based on the result of a Kolmogorov-Smirnov (K-S) test, a ANOVA test was employed for testing H′ and j′.

after the dam), and prasinophytes (outer zone). This summer bloom was consistent with prior findings (Sin et al., 2015; Kim and Shin, 2021; Park and Sin, 2022). The close relationship between Chl a and temperature in the CCA plot (Figure 8B), separated from higher DIN concentrations, indicates that intensive discharge in summer caused the mismatch between the supply and consumption of nutrients in the phytoplankton community.

In autumn, the two estuaries are concurrently characterized by the overwhelming dominance of diatoms (>70%). Our ANOSIM and SIMPER analyses revealed subtle (average dissimilarity = 18.0) but significant differences (Global R = 0.759) that cannot be explained by the overall differences in phytoplankton composition between the two estuaries due to the high contribution of diatoms (Figure 2). The diatom dominance was explained by the seasonal cycle of abiotic conditions on the western coast of Korea, which included enhanced mixing in the water column due to tidal activity and seasonally strengthened winds, an adequate temperature range (15°C–20°C) (Kang et al., 2019), and thus replete conditions of DIN (see Figures 5A–E). Considering the tidal flat as a source of inorganic nutrients, NH_4^+ can be replenished by re-mineralization during summer and autumn and then exported offshore through active tidal mixing (Kim et al., 2011). High concentrations of NH_4^+ and DIP were observed in autumn and summer during the study period. Nitrogen from nonpoint sources may also be utilized by phytoplankton flowing from adjacent cities (e.g., Incheon Harbor for the HRE and Mokpo Harbor for the YRE). This is supported by the lack of a close relationship between NH_4^+ and salinity in the CCA plot (see Figures 8A, B). In an urbanized estuary, NH_4^+ can remain at concentrations sufficient to inhibit NO_3^- uptake when the flow is sufficiently high in the channel, stimulating diatom dominance (Dugdale et al., 2012).

Notably, conspicuous dissimilarities of phytoplankton community structure were observed in winter. Specifically, the HRE manifested remarkable differences in both seasonal (e.g., autumn and spring) and inter-estuarine comparisons, which were

characterized by increasing diatoms and cryptophytes. During winter, dry conditions related to low precipitation minimize riverine flushing, thereby strengthening the effect of seawater intrusion through tidal mixing in the HRE (Lim et al., 2007; Lee et al., 2021). In addition, strong wind and tidal currents may form highly turbid conditions by resuspension of sediments, resulting in low light availability in the HRE (Park, 2007). Given seawater-dominant conditions, wind-driven current from the YS can supply NO_3^- via the Korean Coastal Current, magnifying the P-limitation in the HRE (Tak et al., 2022). Consequently, cryptophytes in the HRE can thrive in winter due to low temperatures, dry atmosphere, and current-driven P-limitation. In contrast to the HRE, the dominance of diatoms lasts from autumn to winter with no obvious change in the phytoplankton community structure in the YRE.

Our study reveals that seasonal changes in the phytoplankton community in the YRE are caused by the contributions of nano- and pico-plankton (e.g., prasinophytes, pelagophytes, prymnesiophytes, and cyanobacteria with Global R > 0.6). This finding is consistent with the community structure of the offshore area in the East/Japan Sea and the Yellow Sea adjacent to the Korea Peninsula. In spring, the abundance of pelagophytes in the YRE differentiated the seasonal and inter-estuarine distributions of the community structure, whereas the seasonal variation in the HRE was minimal. Pelagophytes are generally considered an oceanic group, and significant contributions of pelagophytes are observed in the Bay of Bengal (Pujari et al., 2019), the Bohai Bay (Wang et al., 2021), and the Korea Peninsula (Kim et al., 2010; Jang et al., 2021). These studies reported negative correlations between pelagophytes and NO_3^-, DSi, and diatoms, which is consistent with our results. A strong tide may deliver offshore water into the two estuaries, and a continuous inflow of freshwater replenishes nutrients in the HRE in contrast to stagnant conditions downstream of the dam in the YRE. In turn, continuous flushing alleviates nutrient limitations, resulting in consecutive phytoplankton community structures, evidenced by the co-occurrence of diatoms and cryptophytes, whereas depletion of nutrients in the stable water column results in the active growth of pelagophytes, tidally transported from offshore. Consequently, the difference in phytoplankton between the two estuaries is attributable to the presence and absence of artificial construction.

In summer, N-limitation was evident in the HRE even though the water column was in a eutrophic condition in terms of the concentration of nutrients. The N-limitation in downstream of continuously flushed by the river was in accordance with previous study conducted in the Seomjin River estuary located in the southern coast of Korea (Lee et al., 2018). Summer bloom in the YRE was followed by an increase in the amount of cyanobacteria and prasinophytes in summer. Notably, increasing nutrient availability was not a limiting factor for phytoplankton growth in the HRE but may influence the growth of phytoplankton during the summer discharging period in the YRE. The contribution of cyanobacteria in the HRE was significant (>20%) after the estuarine dam (MP1) and gradually decreased toward the open sea during summer, whereas that in the HRE was negligible. Cyanobacteria are competitive within the temperature range of 25°C–35°C (Lürling et al., 2013). Previous studies have reported

that cyanobacteria can be a dominant phytoplankton group upstream of estuarine dams on the western coast of Korea because of the increased retention time, resulting in nutrient depletion (Sin et al., 2015; Kim et al., 2021b). Given that there is no significant difference in seawater temperatures between the two estuaries, cyanobacteria flourished in the YRE during summer because of a combination of optimal growth temperature and physical input through dam discharge water. A previous study demonstrated that opening the middle stream weir and estuarine dam in the Yeongsan River reduced the magnitude of summer cyanobacteria blooms by regulating the reservoir retention time (Kim and Shin, 2021). Furthermore, the opening of the dam and weir in the Yeongsan River reduced the magnitude and frequency of algal blooms, which is similar to the lack of obvious seasonality of the Chl a concentration in this study (Kim and Shin, 2021). This suggests that the estuarine dam influences the phytoplankton community structure by allowing drifting cyanobacterial to enter the dam through the sluice gate (Doi et al., 2008).

4.2 Phenology of diatoms and cryptophytes

During the study period, the two estuaries were characterized by diatom dominance and phytoplankton communities distinguished by small phytoplankton populations (e.g., cryptophytes, prasinophytes, pelagophytes, and cyanobacteria), inducing the inter-estuarine dissimilarity of the phytoplankton community. Ubiquitous characteristics of diatoms are consistently observed in estuaries in the temperate zone, such as the marginal zone of the Yellow Sea (Zhou et al., 2008; Kim et al., 2023). Diatoms were the most prevalent group, owing to the well-mixed condition of shallow estuaries in the temperate zone (Mallin et al., 1991; Trigueros and Orive, 2001; Haese et al., 2007). Indeed, the increases in contributions of diatoms and cryptophytes were observed in the estuaries in the Nakdong River and the Geum River, which are major rivers in terms of dranage in Korea (Baek et al., 2019; Kim et al., 2019; Kim et al., 2023). This study showed the prevalence of diatoms in community composition (> 40%) throughout the year on the western coast of Korea. The results are consistent with previous reports, implying the dominance of diatoms under well-mixed conditions due to tidal mixing on the western coast of Korea (Park et al., 2022). Despite the limitation of the CHEMTAX method for depicting the phytoplankton community structure, which can only provide groups at the class level, the negative relationship between diatom contribution (%) and α-indices (e.g., Shannon–Wiener diversity index and Pielou evenness index) indicates that the regulation of the community structure on the western coast of Korea is strongly associated with the phenology of diatoms (Supplementary Figures 1A, B).

Cryptophytes were the second most prevalent group among the phytoplankton community structures in the HRE. Previous studies have revealed a positive correlation between cryptophytes and nitrate loading, resulting from P-limitation in estuarine areas in Korea (Bibi et al., 2020) and the eastern coast (Kang et al., 2021), characterized by continuous flushing of riverine input. Our CCA

results explained the thriving of cryptophytes in the HRE with nitrate-associated DIN concentrations.

The swing of diatoms and cryptophytes was evident in the study area (Figure 8 and Supplementary Figure 1C). The negative correlation between these two groups is evidenced in our CCA results in both the HRE and YRE (Figures 8A, B). This result is consistent with previous reports on temperate estuaries (Kang et al., 2021; Santos et al., 2022). Several studies have presented reasons for the increase in cryptophyte dominance in estuaries with P-limitation (Hyun et al., 2011; Santos et al., 2022), such as seasonal variations in environmental conditions, grazing impact of shellfish, and climate change (Jahan and Choi, 2014). For example, diatom–small flagellate alternation is typical on the Mediterranean coasts, characterized by the dominance of cryptophytes associated with well-mixed conditions under lower light availability during winter (Zingone et al., 2010; D'Alelio et al., 2015). Given that the HRE has a higher concentration of total suspended solids (TSS) than the YRE, which is governed by freshwater runoff (Park, 2007), the enhanced contribution of cryptophytes during winter supports the contrast structure between the HRE and YRE in terms of the phenology of cryptophytes (Figures 3C, D). In addition to the thriving of cryptophytes, the recently declining concentration of nitrogenous nutrients but increasing N:P ratio by water quality control, referred to as "P-only strategy," presumably leads to a dramatic swing of diatoms and cryptophytes, reflecting the DIN regulation of the phytoplankton community structure in long-run (Kim et al., 2021a).

4.3 Ecological implications: the impact of estuarine dam

The western coast of Korea has recently experienced changes in physicochemical conditions such as winter warming of the surface seawater (Jahan and Choi, 2014; Park et al., 2015) and an increase/decrease in the amount of dissolved nutrients (Park et al., 2023). The response of macrotidal estuaries to nitrogen loading differs, which is mainly regulated by sediment resuspension, and thus, increasing turbidity hinders the active consumption of nutrients (Monbet, 1992). Kim et al. (2017) reported similar seasonality between Chl a concentration and TSS in the Gyeonggi Bay (the HRE) and the southwestern coast of Korea (adjacent to the YRE), which are profoundly affected by tidal currents. As these coastal areas are characterized by shallow continental shelves, the tide-dominant environment is vulnerable to changes in physical conditions, which can cause different responses of the phytoplankton community structure by determining the magnitude of energy transport from organic matter derived from phytoplankton along the coastal processes (Najjar et al., 2010; Hwang et al., 2014; Lee et al., 2022). Our study supports the vulnerability of the phytoplankton community structure in shallow macrotidal estuaries due to increased differences during winter combined with macrotidal conditions, strengthened monsoonal winds, and minimized freshwater input. Considering this evident difference in the phytoplankton community structure in winter, climatic changes in winter (e.g., increasing seawater

temperature and precipitation) can cause unpredictable changes in the ecosystem structure (Najjar et al., 2010). Along with climatic changes, long-term variations in the nutrient concentration and ratios may influence the phytoplankton community structure, for example, increasing N:P ratio and declining total nitrogen downstream in the Han River, in contrast to the increasing DIN concentration in the Yeongsan River. Pinckney et al. (2020) reported 25 µM as the DIN breakpoint for phytoplankton group diversity in high-saline coastal water (22–36 salinity), with the following unpredictability above this breakpoint. Despite spatial variability in DIN breakpoints, the long-term trend of increasing DIN suggests that the eutrophication of coastal areas in Korea may cause a shift in the phytoplankton community structure.

Damming of rivers is considered a cataclysmic event in the riverine ecosystem because it disconnects habitats from secondary and primary producers in the coastal ecosystem such as filter-feeding bivalve and fish larvae (Ligon et al., 1995; Lee et al., 2022). Flushing serves as a regulator of phytoplankton and its consumer in lower estuaries by controlling salinity, light availability, and material retention time and/or by enhancing/reducing nutrient limitations (Schöne et al., 2003; Murrell et al., 2007). The case of the Three Gorges Dam, which is connected to the East China Sea, the world's largest hydroelectric construction, may well explain the impact of dams, implying the alternation of estuaries with high variability in the microbial structure depending on dam discharge (Jiao et al., 2007). Our study shows the flourishing of cyanobacteria near the dam in summer, presumably transported from dam discharge. Considering the possible contribution of reservoir plankton to nitrogen uptake by consumers as a form of fine particulate organic matter, cyanobacteria can supply trophic subsidy to the coastal food web through dam discharge (Doi et al., 2008; Ock and Takemon, 2014). The pelagic food web structure can be shifted by changing the dominant phytoplankton (diatoms–cryptophytes–cyanobacteria), which can be triggered by variability in dominant forms and nutrient amounts and ratios through the phytoplankton community structure (Glibert, 2010). Cryptophytes have a low biovolume; thus, increasing their dominance may be insufficient to compensate for the loss of diatom contribution in terms of energy transfers from primary producers to higher-trophic-level organisms (Lehman et al., 2010). Therefore, the presence of an estuarine dam can cause a shift in the downstream ecosystem via bottom-up regulation of phytoplankton initiated by the discontinuity of riverine–estuarine–coastal continuum, whereas the contribution of small-size phytoplankton is enhanced by water quality treatment of nutrients, intensifying P-limitation on the western coast of Korea.

5 Conclusions

A mechanism that describes seasonal variability in the phytoplankton community structure has been explained in relation to the role of freshwater inflow and estuarine dams on the western coast of Korea (Sin et al., 2013; Kim et al., 2023). Our study explored the seasonal succession of phytoplankton and

spatially compared the phytoplankton community structure to understand the impact of the presence or absence of a dam in two estuaries on the western coast of Korea. Hydrographic properties reflected the prevalence of freshwater runoff and seawater intrusion in a natural estuary in contrast to the summer perturbation of DIN from discharge water in a dammed estuary on the western coast of Korea. Diatoms were the dominant phytoplankton group during the study period, determining the diversity and evenness of phytoplankton on the western coast of Korea. The occurrence of cryptophytes in the natural estuary indicates that freshwater input serves as a regulator of stoichiometric ratios and nutrient availability. We observed a significant difference in the phytoplankton community structure between the two estuaries during winter, which was mainly determined by the enhanced contribution of cryptophytes in the natural estuary, whereas diatoms remained the dominant group in the water column. This suggests that the combination of strengthened wind and active tidal mixing on the western coast of Korea maximizes the adapting mechanisms of cryptophytes under turbid conditions with continuous DIN input through the river continuum even though the impact of riverine input is minimized during the dry season. The drastic increase in cyanobacteria associated with a phytoplankton bloom in the dammed estuary suggests that an estuarine dam serves multiple functions, including nutrient regulators, nutrient suppliers, and physical transportation of the dominant phytoplankton group into an estuary. Our study provides a baseline for future research to understand ecological responses to the impoundment of dams in terms of bottom-up regulation in macrotidal estuaries.

Data availability statement

The original contributions presented in the study are included in the article/Supplementary Material. Further inquiries can be directed to the corresponding author.

Ethics statement

The manuscript presents research on animals that do not require ethical approval for their study.

Author contributions

DK: Data curation, Formal Analysis, Methodology, Writing – original draft, Writing – review & editing. JWS: Investigation, Methodology, Writing – original draft. THK: Conceptualization, Data curation, Writing – review & editing. HMC: Conceptualization, Validation, Writing – review & editing. JK: Data curation, Validation, Writing – review & editing. HJP: Conceptualization, Data curation, Supervision, Writing – original draft, Writing – review & editing.

Funding

Conflict of interest

The authors declare that the research was conducted in the absence of any commercial or financial relationships that could be construed as a potential conflict of interest.

Publisher's note

All claims expressed in this article are solely those of the authors and do not necessarily represent those of their affiliated organizations, or those of the publisher, the editors and the reviewers. Any product that may be evaluated in this article, or claim that may be made by its manufacturer, is not guaranteed or endorsed by the publisher.

Supplementary material

The Supplementary Material for this article can be found online at: https://www.frontiersin.org/articles/10.3389/fmars.2023.1257904/full#supplementary-material

References

Baek, S. H., Kim, D., Kim, Y. O., Son, M., Kim, Y. J., Lee, M., et al. (2019). Seasonal changes in abiotic environmental conditions in the Busan coastal region (South Korea) due to the Nakdong River in 2013 and effect of these changes on phytoplankton communities. *Cont. Shelf Res.* 175, 116–126. doi: 10.1016/j.csr.2019.01.014

Bibi, R., Kang, H. Y., Kim, D., Jang, J., Kundu, G. K., Kim, Y. K., et al. (2020). Dominance of autochthonous phytoplankton-derived particulate organic matter in a low-turbidity temperate estuarine embayment, Gwangyang Bay, Korea. *Front. Mar. Sci.* 7. doi: 10.3389/fmars.2020.580260

Bray, J. R., and Curtis, J. T. (1957). An ordination of the upland forest communities of southern Wisconsin. *Ecol. Monogr.* 27 (4), 326–349. doi: 10.2307/1942268

Byun, D. S., Wang, X. H., and Holloway, P. E. (2004). Tidal characteristic adjustment due to dyke and seawall construction in the mokpo coastal zone, korea. *Estuar. Coast. Shelf Sci.* 59 (2), 185–196. doi: 10.1016/j.ecss.2003.08.007

Cho, Y. K., Park, L. H., Cho, C., Lee, I. T., Park, K. Y., and Oh, C. W. (2004). Multi-layer structure in the Youngsan Estuary, Korea. *Estuar. Coast. Shelf Sci.* 61 (2), 325–329. doi: 10.1016/j.ecss.2004.06.003

Choi, J. W., Kim, H. D., and Wang, B. (2020). Interdecadal variation of Changma (Korean summer monsoon rainy season) retreat date in Korea. *Int. J. Climatol.* 40 (3), 1348–1360. doi: 10.1002/joc.6272

Cloern, J. E., and Jassby, A. D. (2010). Patterns and scales of phytoplankton variability in estuarine–coastal ecosystems. *Estuar. Coast.* 33, 230–241. doi: 10.1007/s12237-009-9195-3

D'Alelio, D., Mazzocchi, M. G., Montresor, M., Sarno, D., Zingone, A., Di Capua, I., et al. (2015). The green–blue swing: plasticity of plankton food-webs in response to coastal oceanographic dynamics. *Mar. Ecol.* 36 (4), 1155–1170. doi: 10.1111/maec.12211

Doi, H., Chang, K. H., Ando, T., Imai, H., Nakano, S. I., Kajimoto, A., et al. (2008). Drifting plankton from a reservoir subsidize downstream food webs and alter community structure. *Oecologia* 156, 363–371. doi: 10.1007/s00442-008-0988-z

Dugdale, R., Wilkerson, F., Parker, A. E., Marchi, A., and Taberski, K. (2012). River flow and ammonium discharge determine spring phytoplankton blooms in an urbanized estuary. *Estuar. Coast. Shelf Sci.* 115, 187–199. doi: 10.1016/j.ecss.2012.08.025

Elliott, M., and McLusky, D. S. (2002). The need for definition in understanding estuaries. *Estuar. Coast. Shelf Sci.* 55, 815–827. doi: 10.1006/ecss.2002.1031

Estrada, M., Latasa, M., Emelianov, M., Gutiérrez-Rodríguez, A., Fernández-Castro, B., Isern-Fontanet, J., et al. (2014). Seasonal and mesoscale variability of primary production in the deep winter-mixing region of the NW Mediterranean. *Deep Sea Res. I* 94, 45–61. doi: 10.1016/j.dsr.2014.08.003

Glibert, P. M. (2010). Long-term changes in nutrient loading and stoichiometry and their relationships with changes in the food web and dominant pelagic fish species in the san francisco estuary, california. *Rev. Fish. Sci.* 18 (2), 211–232. doi: 10.1080/10641262.2010.492059

Gomez, F. A., Lee, S. K., Hernandez, F. J.Jr., Chiaverano, L. M., Muller-Karger, F. E., Liu, Y., et al. (2019). ENSO-induced co-variability of salinity, plankton biomass and coastal currents in the Northern Gulf of Mexico. *Sci. Rep.* 9 (1), 178. doi: 10.1038/s41598-018-36655-y

Haese, R. R., Murray, E. J., Smith, C. S., Smith, J., Clementson, L., and Heggie, D. T. (2007). Diatoms control nutrient cycles in a temperate, wave-dominated estuary

(southeast Australia). *Limnol. Oceanogr.* 52 (6), 2686–2700. doi: 10.4319/lo.2007.52.6.2686

Hansen, H. P., and Grasshoff, K. (1983). "Procedures for the automated determination of seawater constituents," in *Methods of seawater analysis, 2nd Ed*. Eds. K. Grasshoff, M. Ehrhardt and K. Kremling (Weinheim: Verlag Chemie), 362–379.

Helder, W., and De Vries, R. T. P. (1979). An automatic phenol-hypochlorite method for the determination of ammonia in sea-and brackish waters. *Netherlands J. Sea Res.* 13 (1), 154–160. doi: 10.1016/0077-7579(79)90038-3

Hong, S., Choi, S. D., and Khim, J. S. (2018). Arsenic speciation in environmental multimedia samples from the Youngsan River Estuary, Korea: A comparison between freshwater and saltwater. *Environ. pollut.* 237, 842–850. doi: 10.1016/j.envpol.2017.11.020

Hwang, J. H., Van, S. P., Choi, B. J., Chang, Y. S., and Kim, Y. H. (2014). The physical processes in the Yellow Sea. *Ocean Coast. Manage.* 102, 449–457. doi: 10.1016/j.ocecoaman.2014.03.026

Hyun, B. G., Shin, K., Kim, D. S., Kim, Y. O., Joo, H. M., and Baek, S. H. (2011). Understanding of phytoplankton community dynamics through algae bioassay experiment during winter season of Janhae bay, Korea. *J. Kor. Soc Oceanogr.* 16 (1), 27–38.

Hyun, J. H., Choi, J. K., Chung, K. H., Yang, E. J., and Kim, M. K. (1999). Tidally induced changes in bacterial growth and viability in the macrotidal han river estuary, yellow sea. *Estuar. Coast. Shelf Sci.* 48 (2), 143–153. doi: 10.1006/ecss.1998.0421

Jäger, C. G., Diehl, S., and Schmidt, G. M. (2008). Influence of water-column depth and mixing on phytoplankton biomass, community composition, and nutrients. *Limnol. Oceanogr.* 53 (6), 2361–2373. doi: 10.4319/lo.2008.53.6.2361

Jahan, R., and Choi, J. K. (2014). Climate regime shift and phytoplankton phenology in a macrotidal estuary: long-term surveys in gyeonggi bay, korea. *Estuar. Coast.* 37, 1169–1187. doi: 10.1007/s12237-013-9760-7

Jang, H. K., Youn, S. H., Joo, H., Kim, Y., Kang, J. J., Lee, D., et al. (2021). First concurrent measurement of primary production in the Yellow Sea, the South Sea of Korea, and the East/Japan Se. *J. Mar. Sci. Eng.* 9 (11), 1237. doi: 10.3390/jmse9111237

Jeffery, S. W., Mantoura, R. F. C., and Wright, S. W. (1997). *Phytoplankton Pigments in Oceanography: Guidelines to Modern Methods* (Paris: UNESCO Publishing), 127–166.

Jiao, N., Zhang, Y., Zeng, Y., Gardner, W. D., Mishonov, A. V., Richardson, M. J., et al. (2007). Ecological anomalies in the East China Sea: impacts of the three gorges dam? *Water Res.* 41 (6), 1287–1293. doi: 10.1016/j.watres.2006.11.053

Jung, T. S., and Choi, J. H. (2010). Numerical modeling of ebb-dominant tidal flow in the mokpo coastal zone. *J. Kor. Soc Coast. Ocean Eng.* 22 (5), 333–343.

Kang, Y., Kang, H. Y., Kim, D., Lee, Y. J., Kim, T. I., and Kang, C. K. (2019). Temperature-dependent bifurcated seasonal shift of phytoplankton community composition in the coastal water off southwestern Korea. *Ocean Sci. J.* 54, 467–486. doi: 10.1007/s12601-019-0025-7

Kang, Y., Moon, C. H., Kim, H. J., Yoon, Y. H., and Kang, C. K. (2021). Water quality improvement shifts the dominant phytoplankton group from cryptophytes to diatoms in a coastal ecosystem. *Front. Mar. Sci.* 8. doi: 10.3389/fmars.2021.710891

Kim, M., Kim, D., Kim, J., Hong, S., and Shin, K. H. (2021b). Distribution of microcystins in environmental multimedia and their bioaccumulation characteristics in marine benthic organisms in the Geum River Estuary, South Korea. *Sci. Total Environ.* 757, 143815. doi: 10.1016/j.scitotenv.2020.143815

Kim, D., Lee, Y. J., Kang, H. Y., Kwon, K. Y., Lee, W. C., and Kwak, J. H. (2019). Seasonal variations in primary productivity and biomass of phytoplankton in Geoje-Hansan Bay on the southern coast of Korea. *Ocean Sci. J.* 54, 213–227. doi: 10.1007/s12601-019-0005-y

Kim, T. H., Lee, Y. W., and Kim, G. (2010). Hydrographically mediated patterns of photosynthetic pigments in the East/Japan Sea: Low N: P ratios and cyanobacterial dominance. *J. Mar. Syst.* 82 (1-2), 72–79. doi: 10.1016/j.jmarsys.2010.03.005

Kim, D., Ji, R., Feng, Z., Jang, J., Lee, D. I., Lee, W. C., et al. (2023). Estuarine dam water discharge enhances summertime primary productivity near the southwestern korean coast. *Mar. pollut. Bull.* 191, 114971. doi: 10.1016/j.marpolbul.2023.114971

Kim, D., Lim, J. H., Chun, Y., Nayna, O. K., Begum, M. S., and Park, J. H. (2021a). Phytoplankton nutrient use and CO2 dynamics responding to long-term changes in riverine N and P availability. *Water Res.* 203, 117510. doi: 10.1016/j.watres.2021.117510

Kim, K. T., Ra, K., Kim, E. S., Yim, U. H., and Kim, J. K. (2011). Distribution of heavy metals in the surface sediments of the Han River and its estuary, Korea. *J. Coast. Res.* 64, 903–907.

Kim, D., and Shin, C. (2021). Algal bloom characteristics of Yeongsan River based on weir and estuary dam operating conditions using EFDC-NIER model. *Water* 13 (16), 2295. doi: 10.3390/w13162295

Kim, H. C., Son, S., Kim, Y. H., Khim, J. S., Nam, J., Chang, W. K., et al. (2017). Remote sensing and water quality indicators in the Korean West coast: Spatio-temporal structures of MODIS-derived chlorophyll-a and total suspended solids. *Mar. pollut. Bull.* 121 (1–2), 425–434. doi: 10.1016/j.marpolbul.2017.05.026

Kwon, K. M., Choi, B. J., Lee, S. H., Cho, Y. K., and Jang, C. J. (2011). Coastal current along the eastern boundary of the yellow sea in summer: numerical simulations. *J. Korean. Soc Oceanogr.* 16 (4), 155–168. doi: 10.7850/jkso.2011.16.4.155

Lee, Y., Choi, D. H., Lee, H., Hyun, M. J., Kim, G., and Lee, H. (2022). Changes in the characteristics of organic matter associated with hydrodynamics and phytoplankton size structure in the central-eastern Yellow Sea. *Sci. Tota Environ.* 807, 151781. doi: 10.1016/j.scitotenv.2021.151781

Lee, H. M., Kim, J. W., Choi, J. Y., Yoon, B. I., and Woo, S. B. (2021). Mechanisms of salt transport in the Han River Estuary, Gyeonggi Bay. *J. Kor. Soc Coast. Ocean Eng.* 33 (1), 13–29. doi: 10.9765/KSCOE.2021.33.1.13

Lee, M., Park, B. S., and Baek, S. H. (2018). Tidal influences on biotic and abiotic factors in the Seomjin River Estuary and Gwangyang Bay, Korea. *Estuar. Coast.* 41, 1977–1993. doi: 10.1007/s12237-018-0404-9

Lee, Y. W., Park, M. O., Kim, Y. S., Kim, S. S., and Kang, C. K. (2011). Application of photosynthetic pigment analysis using a HPLC and CHEMTAX program to studies of phytoplankton community composition. *J. Korean Soc Oceanogr.* 16, 117–124. doi: 10.7850/jkso.2011.16.3.117

Lehman, P. W., Teh, S. J., Boyer, G. L., Nobriga, M. L., Bass, E., and Hogle, C. (2010). Initial impacts of *Microcystis aeruginosa* blooms on the aquatic food web in the San Francisco Estuary. *Hydrobiologia* 637, 229–248. doi: 10.1007/s10750-009-9999-y

Ligon, F. K., Dietrich, W. E., and Trush, W. J. (1995). Downstream ecological effects of dams. *Bioscience* 45 (3), 183–192. doi: 10.2307/1312557

Lim, D. I., Rho, K. C., Jang, P. G., Kang, S. M., Jung, H. S., Jung, R. H., et al. (2007). Temporal-spatial variations of water quality in Gyeonggi Bay, west coast of Korea, and their controlling factor. *Ocean Polar Res.* 29 (2), 135–153. doi: 10.4217/OPR.2007.29.2.135

Lürling, M., Eshetu, F., Faassen, E. J., Kosten, S., and Huszar, V. L. (2013). Comparison of cyanobacterial and green algal growth rates at different temperatures. *Freshw. Biol.* 58 (3), 552–559. doi: 10.1111/j.1365-2427.2012.02866.x

Mackey, M. D., Mackey, D. J., Higgins, H. W., and Wright, S. W. (1996). CHEMTAX-a program for estimating class abundances from chemical markers: application to HPLC measurements of phytoplankton. *Mar. Ecol. Prog. Ser.* 144, 265–283. doi: 10.3354/meps144265

Mallin, M. A., Paerl, H. W., and Rudek, J. (1991). Seasonal phytoplankton composition, productivity and biomass in the Neuse River estuary, North Carolina. *Estuar. Coast. Shelf Sci.* 32 (6), 609–623. doi: 10.1016/0272-7714(91)90078-P

Monbet, Y. (1992). Control of phytoplankton biomass in estuaries: a comparative analysis of microtidal and macrotidal estuaries. *Estuaries* 15, 563–571. doi: 10.2307/1352398

Morris, R. K. (2013). Geomorphological analogues for large estuarine engineering projects: a case study of barrages, causeways and tidal energy projects. *Ocean Coast. Manage.* 79, 52–61. doi: 10.1016/j.ocecoaman.2012.05.010

Murphy, J., and Riley, J. P. (1962). A modified single solution method for the determination of phosphate in natural waters. *Anal. Chim. Acta* 27, 31–36. doi: 10.1016/S0003-2670(00)88444-5

Murrell, M. C., Hagy, J. D., Lores, E. M., and Greene, R. M. (2007). Phytoplankton production and nutrient distributions in a subtropical estuary: importance of freshwater flow. *Estuar. Coast.* 30, 390–402. doi: 10.1007/BF02819386

Najjar, R. G., Pyke, C. R., Adams, M. B., Breitburg, D., Hershner, C., Kemp, M., et al. (2010). Potential climate-change impacts on the chesapeake bay. *Estuar. Coast. Shelf Sci.* 86 (1), 1–20. doi: 10.1016/j.ecss.2009.09.026

Ock, G., and Takemon, Y. (2014). Effect of reservoir-derived plankton released from dams on particulate organic matter composition in a tailwater river (Uji River, Japan): source partitioning using stable isotopes of carbon and nitrogen. *Ecohydrology* 7 (4), 1172–1186. doi: 10.1002/eco.1448

Paerl, H. W. (2006). Assessing and managing nutrient-enhanced eutrophication in estuarine and coastal waters: Interactive effects of human and climatic perturbations. *Ecol. Eng.* 26 (1), 40–54. doi: 10.1016/j.ecoleng.2005.09.006

Park, G. S. (2007). The role and distribution of total suspended solids in the macrotidal coastal waters of Korea. *Environ. Monit. Assess.* 135, 153–162. doi: 10.1007/s10661-007-9640-3

Park, H. B., Kang, K., Lee, G. H., and Shin, H. J. (2012). Distribution of salinity and temperature due to the freshwater discharge in the Yeongsan Estuary in the summer of 2010. *J. Kor. Soc Oceanogr.* 17 (3), 139–148. doi: 10.7850/jkso.2012.17.3.139

Park, S., Kim, G., Kwon, H. K., and Han, I. S. (2023). Long-term changes in the concentrations of nutrients in the marginal seas (Yellow Sea, East China Sea, and East/Japan Sea) neighboring the Korean Peninsula. *Mar. pollut. Bull.* 192, 115012. doi: 10.1016/j.marpolbul.2023.115012

Park, M. O., and Park, J. S. (1997). HPLC method for the analysis of chlorophylls and carotenoids from marine phytoplankton. *J. Kor. Soc Oceanogr.* 32 (1), 46–55.

Park, K. A., Lee, E. Y., Chang, E., and Hong, S. (2015). Spatial and temporal variability of sea surface temperature and warming trends in the Yellow Sea. *J. Mar. Syst.* 143, 24–38. doi: 10.1016/j.jmarsys.2014.10.013

Park, J. S., Lee, K. W., Jung, S. W., Lee, T. K., and Joo, H. M. (2022). Winter distribution of diatom assemblages along the coastline of R.O. Korea in 2010. *Acta Oceanol. Sin.* 41 (6), 68–77. doi: 10.1007/s13131-021-1929-5

Park, K., Oh, J. H., Kim, H. S., and Im, H. H. (2002). Case study: mass transport mechanism in Kyunggi Bay around Han River mouth, Korea. *J. Hydrau. Eng.* 128 (3), 257–267. doi: 10.1061/(ASCE)0733-9429(2002)128:3(257

Park, S., and Sin, Y. (2022). Charactecphyll-a in the seawater zone of the Yeongsan River Estuary: Long-term, (2009–2018) data analysis. *Ocean Polar Res.* 44 (1), 13–27. doi: 10.4217/OPR.2022001

Pinckney, J. L., Knotts, E. R., Kibler, K. J., and Smith, E. M. (2020). Nutrient breakpoints for estuarine phytoplankton communities. *Limnol. Oceanogr.* 65 (12), 2999–3016. doi: 10.1002/lno.11570

Pritchard, D. W. (1967). *What Is An Estuary: Physical Viewpoint* Vol. 1. Ed. G. H. Lauff (Washington DC: Estuaries, American Association for the Advancement of Science), 149–176.

Prowe, A. F., Pahlow, M., Dutkiewicz, S., Follows, M., and Oschlies, A. (2012). Top-down control of marine phytoplankton diversity in a global ecosystem model. *Prog. Oceanogr.* 101 (1), 1–13. doi: 10.1016/j.pocean.2011.11.016

Pujari, L., Wu, C., Kan, J., Li, N., Wang, X., Zhang, G., et al. (2019). Diversity and spatial distribution of chromophytic phytoplankton in the bay of Bengal revealed by RuBisCO genes (rbc L). *Front. Microbiol.* 10. doi: 10.3389/fmicb.2019.01501

Santos, M., Amorim, A., Brotas, V., Cruz, J. P. C., Palma, C., Borges, C., et al. (2022). Spatio-temporal dynamics of phytoplankton community in a well-mixed temperate estuary (Sado Estuary, Portugal). *Sci. Rep.* 12 (1), 16423. doi: 10.1038/s41598-022-20792-6

Schöne, B. R., Flessa, K. W., Dettman, D. L., and Goodwin, D. H. (2003). Upstream dams and downstream clams: growth rates of bivalve mollusks unveil impact of river management on estuarine ecosystems (Colorado River Delta, Mexico). *Estuar. Coast. Shelf Sci.* 58 (4), 715–726. doi: 10.1016/S0272-7714(03)00175-6

Seung, Y. H., Chung, J., ,. H., and Park, Y. C. (1990). Oceanographic studies related to the tidal front in the mid-Yellow Sea off Korea: Physical aspects. *J. Kor. Soc Oceanogr.* 25 (2), 84–95.

Shin, H. J., Lee, G. H., Kang, K., and Park, K. (2019). Shift of estuarine type in altered estuaries. *Anthropocene Coasts* 2 (1), 145–170. doi: 10.1139/anc-2018-0013

Sin, Y., Hyun, B., Jeong, B., and Soh, H. Y. (2013). Impacts of eutrophic freshwater inputs on water quality and phytoplankton size structure in a temperate estuary altered by a sea dike. *Mar. Environ. Res.* 85, 54–63. doi: 10.1016/j.marenvres.2013.01.001

Sin, Y., Lee, E., Lee, Y., and Shin, K. H. (2015). The river–estuarine continuum of nutrients and phytoplankton communities in an estuary physically divided by a sea dike. *Estuar. Coast. Shelf Sci.* 163, 279–289. doi: 10.1016/j.ecss.2014.12.028

Smayda, T. J., and Reynolds, C. S. (2001). Community assembly in marine phytoplankton: application of recent models to harmful dinoflagellate blooms. *J. Plankton Res.* 23 (5), 447–461. doi: 10.1093/plankt/23.5.447

Tak, Y. J., Cho, Y. K., Hwang, J., and Kim, Y. Y. (2022). Assessments of nitrate budgets in the Yellow Sea based on a 3D physical-biogeochemical coupled model. *Front. Mar. Sci.* 8. doi: 10.3389/fmars.2021.785377

Ter Braak, C. J. F., and Smilauer, P. (2002). CANOCO reference manual and CanoDraw for Windows user's guide: software for canonical community ordination (version 4.5). (Ithaca, New York, USA: Biometris Wageningen). Available at: www.canoco.com.

Trigueros, J. M., and Orive, E. (2001). Seasonal variations of diatoms and dinoflagellates in a shallow, temperate estuary, with emphasis on neritic assemblages. *Hydrobiologia* 444, 119–133. doi: 10.1023/A:1017563031810

Wang, Y., Hu, X., Sun, Y., and Wang, C. (2021). Influence of the cold bottom water on taxonomic and functional composition and complexity of microbial communities in the southern yellow sea during the summer. *Sci. Total Environ.* 759, 143496. doi: 10.1016/j.scitotenv.2020.143496

Wolanski, E., and Elliot, M. (2016). *Estuarine Ecohydrology* (Amsterdam, NL: Elsevier).

Wright, S. W., Thomas, D. P., Marchant, H. J., Higgins, H. W., Mackey, M. D., and Mackey, D. J. (1996). Analysis of phytoplankton of the australian sector of the southern ocean: comparisons of microscopy and size frequency data with interpretations of pigment HPLC data using the 'CHEMTAX' matrix factorisation program. *Mar. Ecol. Prog. Ser.* 144, 285–298. doi: 10.3354/meps144285

Yoon, B. I., and Woo, S. B. (2013a). Tidal asymmetry and flood/ebb dominance around the Yeomha channel in the Han River Estuary, South Korea. *J. Coast. Res.* 65 (10065), 1242–1246. doi: 10.2112/SI65-210.1

Yoon, B. I., and Woo, S. B. (2013b). Correlation between freshwater discharge and salinity intrusion in the Han River Estuary, South Korea. *J. Coast. Res.* 65 (10065), 1247–1252. doi: 10.2112/SI65-211.1

Yoon, B. I., and Woo, S. B. (2015). The along-channel salinity distribution and its response to river discharge in tidally-dominated Han River Estuary, South Korea. *Proc. Eng.* 116, 763–770. doi: 10.1016/j.proeng.2015.08.362

Youn, S. H., and Choi, J. K. (2008). Distribution pattern of zooplankton in the Han River estuary with respect to tidal cycle. *Ocean Sci. J.* 43, 135–146. doi: 10.1007/BF03020694

Zapata, M., Rodríguez, F., and Garrido, J. L. (2000). Separation of chlorophylls and carotenoids from marine phytoplankton: a new HPLC method using a reversed phase C8 column and pyridine-containing mobile phases. *Mar. Ecol. Prog. Ser.* 195, 29–45. doi: 10.3354/meps19502

Zhou, M. J., Shen, Z. L., and Yu, R. C. (2008). Responses of a coastal phytoplankton community to increased nutrient input from the Changjiang (Yangtze) River. *Cont. Shelf Res.* 28 (12), 1483–1489. doi: 10.1016/j.csr.2007.02.009

Zingone, A., Dubroca, L., Iudicone, D., Margiotta, F., Corato, F., Ribera d'Alcalà, M., et al. (2010). Coastal phytoplankton do not rest in winter. *Estuar. Coast.* 33, 342–361. doi: 10.1007/s12237-009-9157-9